

First-principles calculations of the magnetic anisotropy energy of Fe-V multilayers

O. Le Bacq, O. Eriksson, and B. Johansson

Condensed Matter Theory Group, University of Uppsala, Box 530, S-751 21 Uppsala, Sweden

P. James

ABB Corporate Research, Västerås, Sweden

A. Delin

*Applied Materials Physics, Department of Materials Science and Engineering, KTH, Brinellvägen 23, 100 44 Stockholm, Sweden
and ICTP, Strada Costiera 11, P.O. Box 586, 34 100 Trieste, Italy*

(Received 23 January 2001; revised manuscript received 27 June 2001; published 25 March 2002)

The magnetic anisotropy energy (MAE) of Fe_2V_6 , Fe_3V_5 , and Fe_4V_4 multilayers are investigated using first-principles spin-polarized and relativistic band-structure calculations based upon the full-potential linearized muffin-tin-orbital method. A strong difference in the MAE and the easy axis of magnetization (calculated for the experimental lattice parameters) is observed between the three studied multilayer systems, with easy axes of (001), (110), and (100) for Fe_2V_6 , Fe_3V_5 , and Fe_4V_4 , respectively. The MAE of the Fe_2V_6 and Fe_4V_4 multilayers agrees well with the experimental data. The origin of this difference of behavior is analyzed, via a study of the influence of the atomic volume as well as a relaxation study of the multilayers with respect to the tetragonal deformation. The important role played by the c/a axial ratio, imposed by the alloying effects, is outlined. The magnetic anisotropy coefficients entering the expression of the MAE, as a function of the directional cosines, are extracted from a series of calculations for four independent spin directions. Finally, the band-filling effects on the MAE are analyzed as well as the different contributions in reciprocal space.

DOI: 10.1103/PhysRevB.65.134430

PACS number(s): 73.40.Jn

I. INTRODUCTION

Materials engineered all the way down to the microscale or even nanoscale open thrilling technological perspectives. A famous example, which quickly found its way into actual application, is magnetic multilayers consisting of repeated slabs of a number of atomic layers of magnetic metals, divided by a spacer material. These artificial materials, although quite simple in their design, exhibit several unique phenomena. One example is antiferromagnetic coupling in a (100) Fe/Cr/Fe sandwich, discovered by Grünberg *et al.*¹ in 1986; another is giant magnetoresistance, first discovered in 1988 by Baibich *et al.*²

The crystallographic direction of the easy axis of magnetization, as well as the magnetic hardness (i.e., how difficult it is to change the magnetization direction), are of fundamental importance for the functionality of these materials. Both these characteristics can be described through the magnetic anisotropy energy (MAE), which has the following definition: the total energy of a magnetic material depends on the direction of magnetization. The energy difference for different directions of magnetization with respect to a reference direction [in this work the (001) direction] is the MAE. Note that here we are only concerned with the contribution due to relativistic effects, as manifested through the spin-orbit coupling. The total easy axis of magnetization for a macroscopic body with a finite extent (i.e., it has a shape) also depends on the shape anisotropy. The latter can be large for, e.g., thin films, but in the experimental data, with which we compare our theory, the shape contribution has been subtracted (see below).

Explicit calculations of the MAE is an attractive but not

so trivial task.^{3–6} Currently, all-electron, full-potential methods within the density-functional theory have strongly contributed to reaching a semiquantitative level for these calculations. Agreement between the theoretical and experimental results for the MAE is generally achieved for the sign and order of magnitude (numerical values may deviate from experiment by a factor of 2) for most of 3d ferromagnets,^{7,8} as well as for monolayers and multilayers containing 3d elements.^{9–13} A noticeable exception is bulk fcc Ni, where, so far, calculations have not been able to reproduce the experimentally observed easy axis.¹⁴

The main goal of the present work is to supply a detailed investigation of the MAE using a highly precise numerical method, with the aim of improving our understanding of how the MAE can be tailored by changing the design of the multilayer. We have chosen to study Fe-V multilayers as a model system for multilayers consisting of a magnetic material with a nonmagnetic transition metal spacer material. An important reason for this choice is that high-quality experimental data exist for several well-characterized Fe-V multilayers, making possible a systematic investigation of how the MAE depends on various design details of the multilayer. Furthermore, no first-principles calculations of the MAE for Fe-V multilayers have yet been published, to our knowledge.

To be specific, we have performed calculations for Fe_2V_6 , Fe_3V_5 , and Fe_4V_4 multilayers. We compare our results with experimental data for the systems $(\text{Fe}_2\text{V}_5)_{60}$ [easy axis (001)] and $(\text{Fe}_4\text{V}_4)_{40}$ [easy axis (100)], which were recently investigated by Farle *et al.*¹⁵ At first sight, our model systems might not appear to be directly comparable to the experimental systems. This point will be clarified in Sec. II, dealing with the details of our calculations.

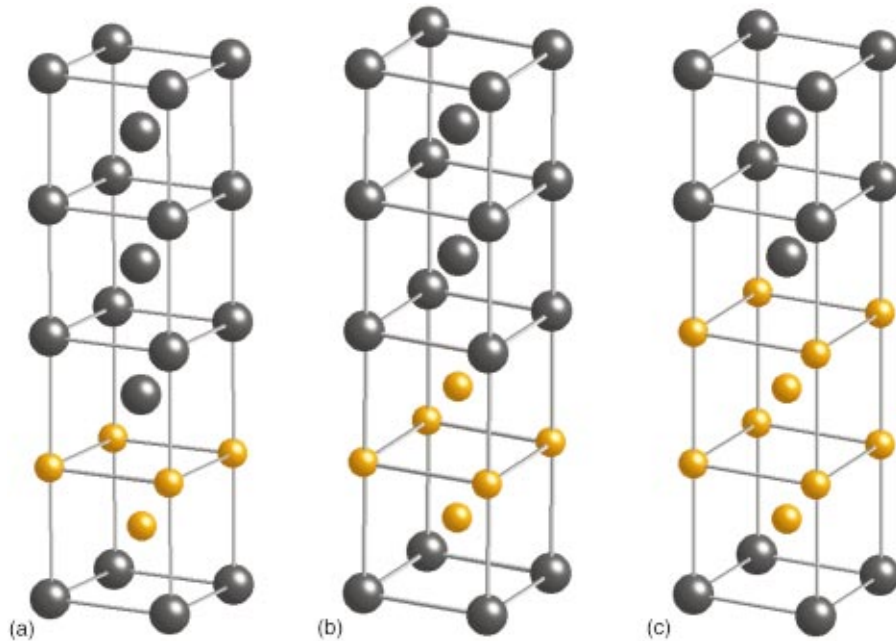


FIG. 1. (Color) Eight-atom bcc supercell used to represent the (a) Fe_2V_6 , (b) Fe_3V_5 , and (c) Fe_4V_4 multilayers. The large and dark atoms are V atoms, and the small ones are Fe atoms.

The presentation of our results is organized as follows. Section III A is devoted to the MAE at the experimental lattice parameters. The directional cosine coefficients, describing the relative hardness of different magnetization directions, are calculated. The MAE is a subtle effect with typical values in the μeV range. Thus it is reasonable to assume that the MAE might be strongly affected by small changes in the structure of the multilayer, e.g., tetragonal deformations and changes in the atomic volume. Section III B is devoted to this question. In reality, the interfaces between the two elements that constitute the multilayer cannot be expected to be perfect, and the exact proportions between the two elements probably also varies slightly from layer to layer. How sensitive is the MAE for changes in the relative proportions of the elements constituting the multilayer? We address this question with a band-filling model in Sec. III C.

II. METHOD OF CALCULATION

A. Total energy calculations

The calculational method used in the present work is the full-potential linearized muffin-tin-orbital (FP-LMTO) method.¹⁶ This method adopts a base geometry based on muffin-tin spheres and an interstitial region. Inside the muffin-tin spheres, the density and potential are expanded by means of spherical harmonic functions times a radial component. In the interstitial region, the expansion of the density and potential are written in the form of a Fourier series, given the fact that the interstitial basis function is a Bloch sum of atomic centered Neumann and Hankel functions displaying the periodicity of the underlying lattice. Thus evaluating the matrix elements of the Hamiltonian in the interstitial region involves relatively simple analytical functions: plane waves. The number of fast Fourier transform coeffi-

cients used to achieve a correct convergence of the wave functions, potential, and charge density in the interstitial region was found to be $20 \times 20 \times 80$. Each Neumann and Hankel function is augmented (or replaced) by a numerical basis function inside the muffin-tin spheres, in the standard way of the linear muffin-tin orbital method.²⁴

The present calculations are all-electron as well as fully relativistic. The latter is achieved by including the mass velocity and Darwin terms in the calculation of the radial functions inside the muffin-tin spheres, whereas the spin-orbit coupling was included at each variational step using an (l, s) basis. Moreover, the present calculations made use of a so-called double basis, which uses two Hankel and Neumann functions each attached to its own radial function for each set of (n, l) quantum numbers. We thus have a set of two $4s$, two $4p$, and two $3d$ orbitals in our expression of the crystal wave function.

The exchange and correlation term is approximated in the present work by the local-spin-density approximation according to the Hedin-Lundqvist parametrization.¹⁷ 1024 \mathbf{k} points were found necessary to achieve the convergence of both the magnetic moments and the self-consistent potentials used as an input to calculate the MAE. The integration in reciprocal space was carried out using the Hermite-Gaussian smearing method¹⁸ with $N=1$ and a smearing parameter $\sigma = 0.02$ Ry. The non-self-consistent calculation of the MAE, using the force theorem, requires specific convergence studies with respect to the number of \mathbf{k} points, that will be described in Sec. III.

We now turn to a closer description of the multilayer systems we have chosen to study. The unit cells of the multilayers are shown in Fig. 1. They are all bcc supercells with eight atomic layers in total. The number of Fe layers range from two to four. We have deliberately chosen to study systems

which can be described by the same type of supercell, setting up the calculation identically, except for the number of V and Fe layers and the choice of the lattice parameters. In this way, it is possible to extract trends from the calculated results. We wish to compare our theoretical results with experimental data, and we also wish to adopt realistic lattice parameters for our multilayers. There exist in the literature, as mentioned in Sec. I, experimental measurements on $(\text{Fe}_2\text{V}_5)_{60}$, $(\text{Fe}_3\text{V}_{13})_{30}$, and $(\text{Fe}_4\text{V}_4)_{40}$, i.e., multilayers. Since the Fe_3V_{13} multilayers cannot be described with a supercell of moderate size, we have eliminated in the calculations the central V layers, which results in a Fe_3V_5 multilayer with the in-plane and out-of-plane lattice parameters being the same as in Fe_3V_{13} . In order to model the Fe_2V_5 multilayer with a periodic supercell, we instead considered Fe_2V_6 , but with the in-plane and out-of-plane lattice constants the same as for Fe_2V_5 . As we shall see below, the approximate multilayers studied theoretically reproduce experiments very well, since the presence of one or several nonmagnetic V layers in the center of the V films does not influence the magnetocrystalline anisotropy, as long as the structural parameters are not modified. In order to mimic the experimental multilayers as closely as possible, we hence adopted the following lattice parameters: the in-plane lattice parameter a_{\parallel} was chosen as 2.97 Å, i.e., the lattice parameter of the (001)-MgO substrate on which the multilayers are grown.^{19–21} The out-of-plane lattice parameters a_{\perp} were chosen to be the experimental values¹⁹ of the $(\text{Fe}_2\text{V}_5)_{60}$, $(\text{Fe}_3\text{V}_5)_{30}$, and $(\text{Fe}_4\text{V}_4)_{40}$ multilayers, namely, 2.931, 2.989, and 2.901 Å for the Fe_2V_6 , Fe_3V_5 , and Fe_4V_4 multilayers, respectively.

B. Force theorem approach

A great deal of theoretical work focused on the calculation of the magnetocrystalline anisotropy energy (MAE), either using the force theorem²² (FT) or the total energy approach (TE). In principle, the FT should be applicable up to linear changes in the charge and magnetization densities, as the magnetization is rotated from one direction to another.²³ Eriksson¹⁴ recently provided numerical evidence that the MAE of 3d elements are rather well reproduced using the FT, and that it gives results similar to TE calculations. Actually, for Fe systems, which are the center of interest in the present work, the difference between the TE and FT calculations of the MAE is smaller than the numerical accuracy of the TE calculations. Motivated by this, the magnetic anisotropy energy $E_a(\sigma)$ was calculated here, using the FT, by an evaluation of the sum of eigenvalues:

$$E_a(\sigma) = \sum_{\mathbf{k},n}^{\text{occ}} \epsilon_{\mathbf{k},n}(\sigma) - \sum_{\mathbf{k},n}^{\text{occ}} \epsilon_{\mathbf{k},n}([001]). \quad (2.1)$$

The expression above states that the MAE is correctly represented by forming the difference of the sum of the occupied eigenvalues of the Hamiltonian taken for the σ and [001] spin directions respectively, provided that the same effective potential is used when the Kohn-Sham equation is solved. This method has the great advantage that only one

nonrelativistic self-consistent calculation of the potential must be done: the energy of another configuration (in our study, when a spin direction, or a c/a ratio, is investigated) is obtained by a single additional (non-self-consistent) relativistic calculation using the previous self-consistent potential. Note that the sign convention we adopted for Eq. (2.1) implies that the easy axis of magnetization of the system is obtained by the σ spin direction which minimizes the $E_a(\sigma)$ function.

Because of the lack of symmetry and the huge number of \mathbf{k} points necessary to achieve convergence of the integrals in the Brillouin zone (BZ) involved in the calculation of the MAE (4056 \mathbf{k} points in the full BZ was found to be necessary for the multilayers and 8000 for the two-atom cell of bcc Fe), a FT approach was used to perform the calculation of the MAE for the four magnetization directions we explored, leading to a considerable gain of time compared to the TE approach. The ability of the FT to predict the MAE of the Fe_4V_4 multilayers was tested by comparing the FT and TE calculations regarding the energy difference between the [100] and [001] spin directions. A value of $-11.5 \mu\text{eV}/\text{atom}$ was obtained with the FT approach, to be compared to the $-15.3 \mu\text{eV}/\text{atom}$ obtained with the TE one. From this, we conclude that the FT approach offers sufficient accuracy, especially concerning trends.

III. RESULTS

A. MAE at experimental lattice parameters

Symmetry considerations dictate that the magnetic anisotropy energy E_a of a tetragonal multilayer system has the form

$$E_a = K_1(\alpha_x^2 + \alpha_y^2) + K_2(\alpha_x^4 + \alpha_y^4) + K_3\alpha_x^2\alpha_y^2 + O(\alpha^6), \quad (3.1)$$

where α_x and α_y are the directional cosines along $\hat{\mathbf{x}}$ and $\hat{\mathbf{y}}$, and the $\hat{\mathbf{z}}$ axis is perpendicular to the plane defined by the layers (basal plane). Provided that the sixth-order corrections can be neglected in Eq. (3.1), the anisotropy coefficients, K_1 , K_2 and K_3 , can be determined by making use of the FT calculation of the MAE [Eq. (2.1)] establishing the total-energy difference between the four quantization directions [001], [100], [110], and [111]:

$$K_1 = -2E_a([110]) + \frac{9}{2}E_a([111]),$$

$$K_2 = E_a([100]) + 2E_a([110]) - \frac{9}{2}E_a([111]), \quad (3.2)$$

$$K_3 = -2E_a([100]) + 8E_a([110]) - 9E_a([111]).$$

The MAE surface, which represents the MAE as a function of the the polar angles (θ, ϕ) defined by $\alpha_x = \sin \theta \cos \phi$, $\alpha_y = \sin \theta \sin \phi$, and $\alpha_z = \cos \theta$, is then finally given by the expression

$$E_a = K_1 \sin^2 \theta + \frac{6K_2 + K_3}{8} \sin^4 \theta + \frac{2K_2 - K_3}{8} \sin^4 \theta \cos 4\phi. \quad (3.3)$$

The calculated values of the magnetic anisotropy energy of the Fe_2V_6 , Fe_3V_5 , and Fe_4V_4 multilayers are given in Table I for the [100], [110], and [111] spin directions. They are calculated at the experimental lattice parameters of the $(\text{Fe}_2\text{V}_5)_{60}$, $(\text{Fe}_3\text{V}_{13})_{30}$, and $(\text{Fe}_4\text{V}_4)_{40}$ multilayers (see Table I for the numerical values). In Table I we also list the corresponding calculated anisotropy coefficients. Apparently, for our systems, the behavior of the MAE is mainly piloted by the K_1 coefficient (compare the value of K_1 with the value of the MAE in the [100] spin direction), since K_2 and K_3 are negligible compared to K_1 . According to Eq. (3.3), the MAE of the three multilayers thus follows a $K_1 \sin^2 \theta$ law, independent of the ϕ angle: the MAE may be considered as homogeneous in the basal plane for the three multilayers. The difference of the MAE between the basal plane, defined by its value in the [100] spin direction, and the reference axis, [001], is thus only determined by the sign and value of the K_1 coefficient. The variation of the MAE with the angle θ is presented in Fig. 2 for the three investigated multilayers. A strong difference is observed in the variation of the MAE with the angle θ . The large value of K_1 for Fe_3V_5 leads to a strong anchoring of the magnetization in the basal plane. The small value of K_1 for Fe_2V_6 does not allow one to find a preferred axis for the magnetization. Fe_4V_4 appears as an intermediate case.

The calculated MAE of Fe_4V_4 ($-11.5 \mu\text{eV}/\text{atom}$) is of the same order of magnitude as the experimental value ($-5 \mu\text{eV}/\text{atom}$).¹⁵ The theoretical value deviates from a factor of two from experiment, which is actually rather typical for first principles theoretical work on MAE.¹⁴ In this particular case, it is also expected that some interdiffusion will affect not only the magnetic moments but also the MAE. As regards the Fe_2V_6 multilayers, the MAE is found to be $2.2 \mu\text{eV}/\text{atom}$. The calculated value is in excellent agreement with the experimental value of the corresponding multilayer, namely, $2.0 \pm 0.5 \mu\text{eV}/\text{atom}$, obtained by Anisimov *et al.*²⁵ with angular-dependent ferromagnetic resonance measurements. For both these multilayers the calculated easy axes, i.e., [001] and [100] for Fe_2V_6 and Fe_4V_4 , respectively, agree with the experiments. No experimental results are available for Fe_3V_5 .

B. Influence of volume and tetragonal deformation

An interesting question is what features of the system actually determine the magnetic anisotropy energy, notably the one between in-plane and out-of-plane magnetizations, or equivalently K_1 . As mentioned in Sec. II, the lattice parameter of the multilayers, imposed by the MgO substrate lattice spacing, induces a large expansion of the atomic volume of the Fe atoms. We carried out a study of the MAE of bct Fe at the atomic volumes and a_{\perp}/a_{\parallel} ratios of the three studied multilayers in order to separate out the influence of hybridization between Fe and V atoms at the interface from effects due to volume and c/a changes of the Fe atoms. The results are shown in Fig. 3. The main characteristic of the plot is that the MAE of bct Fe decreases as the volume (or the a_{\perp}/a_{\parallel} ratio, a_{\parallel} being fixed) increases. The MAE of bct Fe, considered at the volume of Fe_2V_6 , remains close to the one of bct

TABLE I. FP-LMTO calculation of the magnetic anisotropy energy of the Fe_2V_6 , Fe_3V_5 , and Fe_4V_4 multilayers calculated for the experimental lattice parameters of the $(\text{Fe}_2\text{V}_5)_{60}$, $(\text{Fe}_3\text{V}_{13})_{30}$, and $(\text{Fe}_4\text{V}_4)_{40}$ multilayers. The results correspond to the difference between the energy of the systems for the $\sigma=[100]$, [110], and [111] spin directions, and the energy for the [001] spin direction, chosen as a reference. The values of the anisotropy coefficients K_1 , K_2 , and K_3 are deduced from the MAE values using the set of equations (3.2).

	Fe_2V_6	Fe_3V_5	Fe_4V_4
a_{\perp}	2.931 ^a	2.989 ^a	2.901 ^a
a_{\parallel}	2.970	2.970	2.970
Magnetic Anisotropy Energy (in $\mu\text{eV}/\text{atom}$)			
$E_a([100])$	2.20	-31.2	-11.5
$E_a([110])$	2.23	-31.5	-10.8
$E_a([111])$	1.48	-20.9	-7.06
Easy axis	[001]	[110]	[100]
expt.	2.0 ± 0.5 ^b [001]	-	-5.0 ^c
Anisotropy Coefficients (in $\mu\text{eV}/\text{atom}$)			
K_1	2.20	-30.9	-10.3
K_2	0.00	-0.21	-1.25
K_3	0.12	-1.74	0.51

^aReference 19.

^bReference 25.

^cReference 15.

Fe at the equilibrium volume of bcc Fe. The easy axis for this atomic volume is found to be the [001] direction (out-of-plane magnetization), just as for the Fe_2V_6 multilayer. At the volume of Fe_3V_5 , bct Fe favors the [110] direction for the easy axis (in-plane magnetization as in the case of the Fe_3V_5 multilayer), whereas, at the volume of Fe_4V_4 , bct Fe favors the [001] direction (out-of-plane magnetization), in contrast to the in-plane magnetization ([100] is the easy axis) that was found for the Fe_4V_4 multilayer. This last result demonstrates that the volume effect of Fe cannot be considered as a single parameter determining the easy axes of these systems, but it certainly does influence the MAE.

Figure 4 gives the MAE of the Fe_2V_6 , Fe_3V_5 , and Fe_4V_4 multilayers for the three [100], [110], and [111] spin directions as a function of the tetragonal deformation. In the calculations, the out-of-plane parameter a_{\perp} was varied from its equilibrium value. The in-plane lattice parameter was adjusted in order to conserve the volume. This calculation at fixed volume allows a direct comparison of our data with the calculation of Eriksson¹⁴ for pure bct Fe, using the same technique and conditions of calculation. The main feature of the variation of the MAE of the three multilayers, as a function of the a_{\perp}/a_{\parallel} ratio, is a deviation from a linear behavior (especially for Fe_4V_4). Figure 4(a) shows, as in the case of bct Fe,¹⁴ that the MAE of Fe_2V_6 increases with a_{\perp}/a_{\parallel} , and that the value of the MAE in the basal plane ($2.2 \mu\text{eV}/\text{atom}$) has the same order of magnitude as the MAE of bct Fe when considered at the same a_{\perp}/a_{\parallel} axial ratio. For Fe_3V_5 [Fig. 4(b)], the variation of the MAE with respect to a_{\perp}/a_{\parallel} is reversed: a decrease of the MAE is observed when a_{\perp}/a_{\parallel}

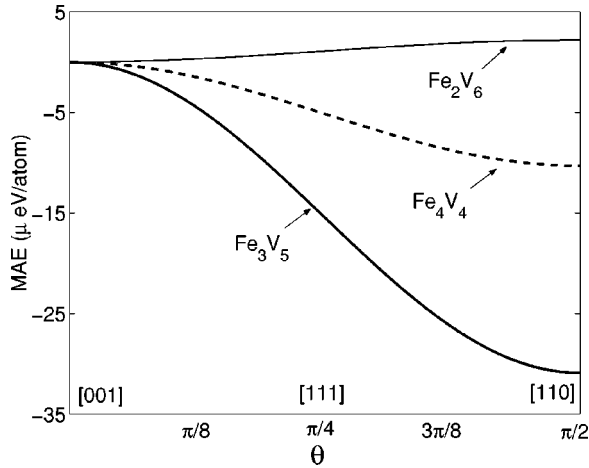


FIG. 2. MAE of the (a) Fe_2V_6 , (b) Fe_3V_5 , and (c) Fe_4V_4 multilayers as a function of the polar angle θ , defined by $\alpha_x = \sin \theta \cos \phi$, $\alpha_y = \sin \theta \sin \phi$, and $\alpha_z = \cos \theta$.

increases. This behavior is consistent with the one of bct Fe when considered at the expanded volume of the multilayers. For Fe_4V_4 , a strong decrease of the MAE is also observed for the largest values of the a_\perp/a_\parallel ratio. This behavior can be considered as normal, given the volume of the multilayer. However, the opposite trend is observed for the lowest values of a_\perp/a_\parallel , and the dependence of the MAE with respect to a_\perp/a_\parallel is very nonlinear. This strong nonlinear behavior of the MAE will be analyzed in the Appendix.

Figure 4(a) shows a small variation of the MAE of Fe_2V_6 in the investigated range of a_\perp/a_\parallel , with an amplitude of the variation of about $5 \mu\text{eV}/\text{atom}$. $E_a(\sigma)$ remains positive for all a_\perp/a_\parallel values, leaving the easy axis, i.e., [001], unchanged. For Fe_3V_5 and Fe_4V_4 the [100] easy axis is found for all values of a_\perp/a_\parallel . For these two systems we find that, the larger the value of the a_\perp/a_\parallel is, the more stable the [100] easy axis. We may also note that for the value of the a_\perp/a_\parallel ratio of the Fe_3V_5 multilayers (1.006), the MAE of Fe_4V_4 reaches the MAE value of Fe_3V_5 in the [100] direction, and that the difference of MAE, $E_a([111]) - E_a([001])$ is equal to $10 \mu\text{eV}/\text{atom}$, to be compared to the value $10.5 \mu\text{eV}/\text{atom}$ obtained for Fe_3V_5 at the same a_\perp/a_\parallel . In other words, the MAE surface of Fe_4V_4 corresponds exactly to the one of Fe_3V_5 , when both systems are considered at the same a_\perp/a_\parallel .

Thus, if very few correlations between the MAE and easy axis of the multilayers were found when we analyzed their discrete values at the experimental lattice parameters (Table I), it seems that we may find a certain agreement and draw general trends via an analysis of their dependence with respect to the a_\perp/a_\parallel ratio. This is especially clear if we compare the MAE of Fe_4V_4 using the a_\perp/a_\parallel ratio of the Fe_3V_5 multilayer. The so-obtained MAE agrees well with the MAE of Fe_3V_5 .

Since the tetragonal a_\perp/a_\parallel ratio is a highly determining and sensitive parameter for the calculation of the MAE, something has to be said here about the mechanisms which determine their equilibrium value in the Fe/V alloys and multilayers. Actually, the equilibrium a_\perp/a_\parallel axial ratio

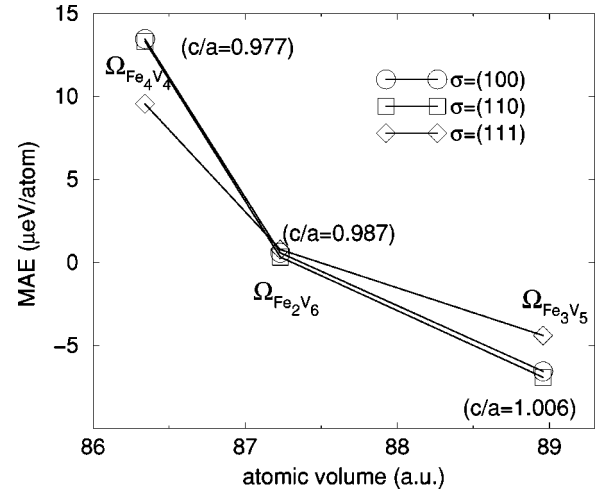


FIG. 3. Magnetic anisotropy energy of bulk bct Fe, calculated at the experimental volume and the c/a axial ratio of the three studied multilayers in the [100], [110], and [111] spin directions.

seems to be imposed by the alloying effects, i.e., it appears that Vegard's law dictates in quite a reliable manner the value of the out-of-plane a_\perp parameter of our multilayers. The calculation of a_\perp using Vegard's law,

$$a_\perp = \frac{n_{\text{Fe}} a_{\text{Fe}} + n_{\text{V}} a_{\text{V}}}{n_{\text{Fe}} + n_{\text{V}}}, \quad (3.4)$$

where a_{Fe} and a_{V} are the equilibrium lattice parameter of pure bcc Fe and bcc V and n_{Fe} and n_{V} are the number of Fe and V layers in the cell, gives values of a_\perp for the Fe_2V_6 , Fe_3V_8 , Fe_3V_{13} , and Fe_4V_4 multilayers, which are compatible with the values observed from the experiments.¹⁹ A small systematic discrepancy of about 0.05 \AA is nevertheless observed for the three systems. Figure 5 illustrates this point by superimposing the experimental and calculated values of a_\perp for the studied multilayers. The main conclusion we may draw from Fig. 5 is that the value of a_\perp satisfies a relationship of proportionality with respect to the lattice parameter of pure Fe and pure V, leading to an increasing value of a_\perp when the fraction of V layers increases (the upper limit being a_{V}). Since the stabilization of the MAE of the multilayers in the basal plane is reinforced by a larger value of a_\perp/a_\parallel , we observe that an increased thickness of the V region, or the choice of another spacer material that presents a larger lattice parameter than the one of V, is expected to produce a strong anchoring of the magnetization in the basal plane.

We end this section with an analysis of the contribution to the calculated MAE from different points in the Brillouin zone. Figure 6 represents the contribution of each \mathbf{k} point to the total MAE of the multilayers in the (k_x, k_y) plane of the reciprocal space, containing the Γ point. The plotted function corresponds to

$$E_a(\mathbf{k}) = \sum_n \omega_{n,\mathbf{k}}^{[100]} \epsilon_n^{[100]}(\mathbf{k}) - \omega_{n,\mathbf{k}}^{[001]} \epsilon_n^{[001]}(\mathbf{k}), \quad (3.5)$$

where ϵ_n^σ is the eigenvalue calculated for the σ spin direction, and $\omega_{n,\mathbf{k}}^\sigma$ is the generalized weight of the \mathbf{k} point, cal-

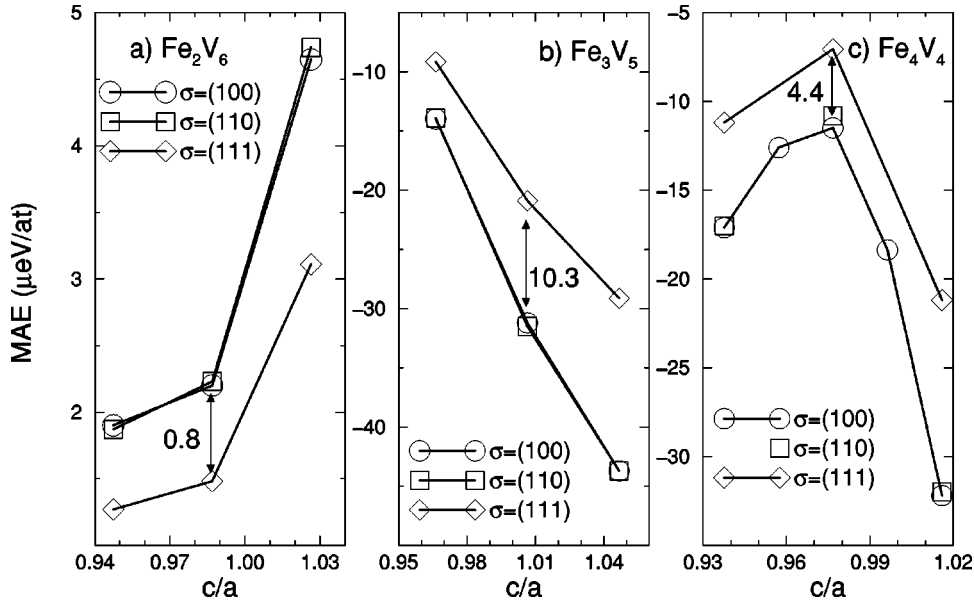


FIG. 4. Magnetic anisotropy energy of the (a) Fe_2V_6 , (b) Fe_3V_5 , and (c) Fe_4V_4 multilayers in the $\sigma=[100]$, $[110]$, and $[111]$ spin directions as a function of the tetragonal deformation defined by the ratio a_{\perp}/a_{\parallel} . The arrows are located at the experimental a_{\perp}/a_{\parallel} ratios of the $(\text{Fe}_2\text{V}_5)_{60}$, $(\text{Fe}_3\text{V}_{13})_{30}$, and $(\text{Fe}_4\text{V}_4)_{40}$ multilayers. Their amplitude gives the difference of the MAE (in $\mu\text{eV}/\text{atom}$) between the basal plane and the $[111]$ crystallographic direction.

culated using the Hermite-Gaussian smearing method. A similar analysis was presented by Wu *et al.*²³ Figures 6(a), 6(b), and 6(c) give the spectral decomposition of the MAE of Fe_4V_4 for $a_{\perp}/a_{\parallel}=0.957$, $a_{\perp}/a_{\parallel}=0.977$, and $a_{\perp}/a_{\parallel}=0.996$, respectively. We observe the following trend: as a_{\perp}/a_{\parallel} increases, the negative contribution from the region, that connects the $\pi/a(1/2,0,0)$ and $\pi/a(0,1/2,0)$ points, expands and increases in magnitude. Moreover, the observed expansion of the negative region moves toward the Γ point, so that the positive region centered on this point is both reduced in magnitude and spatial extent. This is particularly noticeable by comparing Eq. (3.5) for $a_{\perp}/a_{\parallel}=0.977$ [Fig. 6(b)] and $a_{\perp}/a_{\parallel}=0.996$ [Fig. 6(c)]. These results are consistent with the evolution of the MAE of Fe_4V_4 with respect to the tetragonal deformation, given in Fig. 4(c). This study also demonstrates that the region of the reciprocal space involved in the change of the MAE of the multilayers with the tetragonal deformation mainly concerns the triangle defined by the Γ , $\pi/a(1/2,0,0)$, and $\pi/a(0,1/2,0)$ points.

C. Band-filling effects

We now proceed with an analysis of how band filling affects the MAE. The eigenvalues of Fe_4V_4 obtained for the $[001]$ and $[100]$ spin directions can be used to estimate the MAE of any Fe-V multilayer, by filling the corresponding densities of state (DOS's), $D^{[001]}(\epsilon)$ and $D^{[100]}(\epsilon)$, with a varying number of electrons, i.e., by varying the Fermi energy. We observed that the MAE remains equal to zero until $E_F=0.45$ Ry (data not shown). This corresponds to a band filling of about 1 electron/atom. Hence, the bottom of the bands brings no contribution to the MAE of these systems. Above $E_F=0.45$ Ry, the $D^{[001]}(\epsilon)$ and $D^{[100]}(\epsilon)$ DOS's are nondegenerate and the MAE is nonvanishing. We are proposing the following model to approximate the band-filling effects in the calculation of the MAE (see the Appendix for a derivation of this equation),

$$E_a(E_F) = \int_{-\infty}^{E_F} \delta N(\epsilon) d\epsilon, \quad (3.6)$$

where $\delta N(\epsilon) = N^{[100]}(\epsilon) - N^{[001]}(\epsilon)$ is the difference of the integrated DOS, evaluated at the energy ϵ . Figure 7 shows the evolution of the MAE of the Fe-V multilayers given by Eq. (3.6). The approximations made in the derivation of Eq. (3.6) introduce a cumulative error of the MAE. This error can be corrected by matching the obtained curve with the value of the MAE of Fe_4V_4 calculated by the FT. The MAE of Fe_2V_6 and Fe_3V_5 were calculated using the FT for a band filling of 46 and 49 electrons per unit cell, respectively, but using the eigenvalues given by the calculation of the self-consistent potential of Fe_4V_4 . The so-obtained points agree with the curve (Fig. 7), demonstrating that the cumulative mistake is correctly compensated for by applying a rigid shift of the curve. The value of the MAE's of Fe_2V_6 , Fe_3V_5 , and Fe_4V_4 , obtained by the exact application of the FT (using the

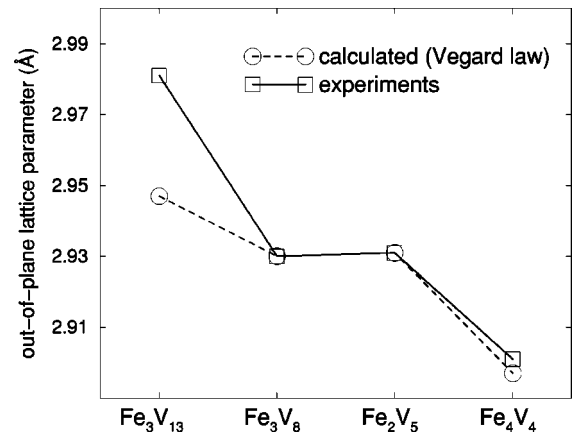


FIG. 5. Comparison between the calculated out-of-plane lattice parameter using the Vegard law, and the experimental values. A translation of -0.05 \AA has been applied to the four points of the calculated set.

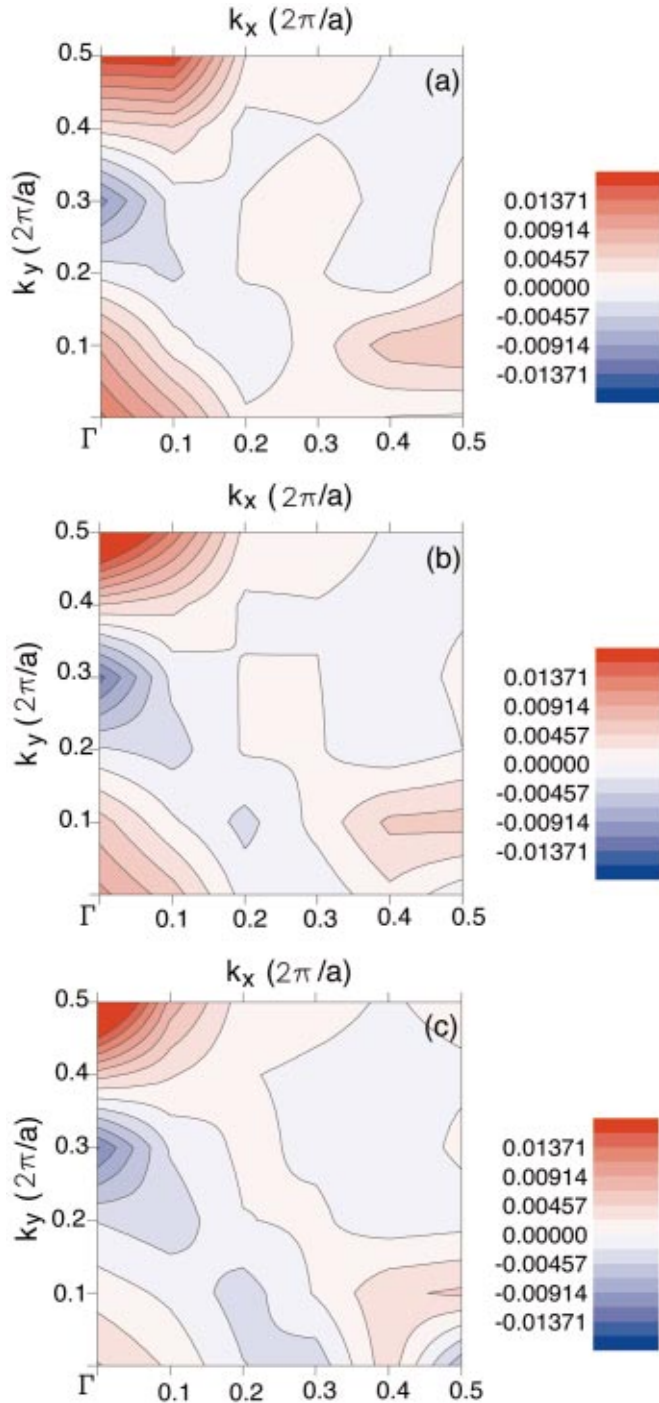


FIG. 6. (Color) Contribution of each \mathbf{k} point to the calculation of the MAE in the (k_x, k_y) plane of the reciprocal space for (a) Fe_4V_4 ($a_\perp/a_\parallel=0.957$), (b) Fe_4V_4 ($a_\perp/a_\parallel=0.977$), and (c) Fe_4V_4 ($a_\perp/a_\parallel=0.996$).

correct eigenvalues) given in Table I, are superimposed at their respective Fermi energy. We attribute the observed discrepancies at the Fermi energy of Fe_2V_6 and Fe_3V_5 to both the difference between the DOS of these multilayers and the one of Fe_4V_4 , and the difference in their volumes (and the a_\perp/a_\parallel ratio) and that of Fe_4V_4 . As expected, the largest discrepancy is obtained for Fe_2V_6 , for which the Fe atoms have the most different atomic environment with respect to Fe_4V_4 .

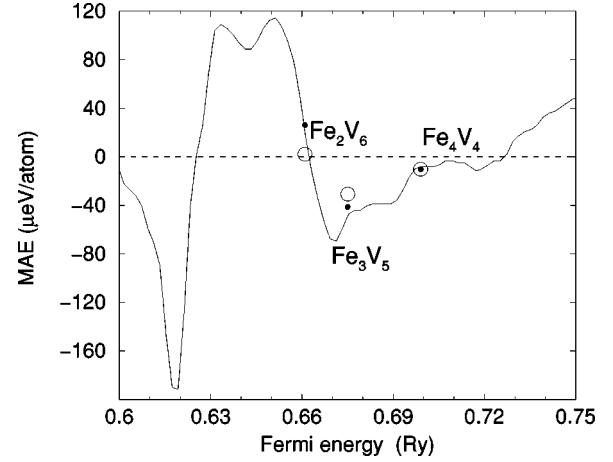


FIG. 7. MAE of the Fe-V multilayers as a function of the Fermi energy, E_F . The exact calculation of the MAE (\circ) is added for a comparison at three band fillings corresponding to Fe_2V_6 , Fe_3V_5 , and Fe_4V_4 . A FT calculation of the MAE using band fillings of 46, 49, and 52 electrons, and the Fe_4V_4 eigenvalue set (\bullet), is added.

Despite these discrepancies, the sign and the value of the MAE of the three studied multilayers agree with the exact calculations. These results demonstrate that band-filling effects determine the value of the MAE of the Fe-V multilayers to a large extent.

This study outlines that the MAE of the Fe-V multilayers depends in a complex manner on the electronic structure, i.e., hybridization effects and band filling. We may easily understand from this that any change in the c/a ratio will affect the electronic structure, and as a consequence, will induce complex changes in the MAE of the multilayers. The strong nonlinear behavior of the MAE with respect to the c/a ratio observed in Fig. 4 has to be understood in this perspective.

IV. SUMMARY

The calculation of the MAE of FeV multilayers was done using the force theorem approach. A complete picture of the MAE landscape as a function of the crystallographic directions was obtained for the experimental values of the lattice parameters, and presented in terms of the anisotropy coefficients K_1 , K_2 , and K_3 . A strong difference in the behavior of the MAE was observed between the three multilayers for these particular crystallographic data, with a strong anchoring of the magnetization in the basal plane for the Fe_3V_5 and Fe_4V_4 multilayers, whereas an out-of-plane easy axis was found for Fe_2V_6 . Our results for Fe_4V_4 and Fe_2V_6 are in agreement with experimental data. However, excellent agreement of the value of the MAE of Fe_2V_6 is somewhat fortuitous, since our calculated spin moments²⁶ deviate to some degree from the experimental data.

A certain coherence between the value and the variation of the MAE with respect to the axial ratio, a_\perp/a_\parallel , was observed and explained by comparing the MAE of the three systems evaluated at various a_\perp/a_\parallel and atomic volumes. This study hence outlines the important role played by the a_\perp/a_\parallel axial ratio as well as the atomic volume and the band-

filling effects on the magnetic anisotropy parameters of the Fe-V multilayers. In addition, the strong hybridization between Fe and V is of great importance not only for the magnetic moments²⁶ but also for the MAE. Also, from a detailed analysis of band-filling effects, we predict that it should be possible to enhance the MAE of FeV multilayers by tuning the Fermi energy to lower values (see Fig.7) either by alloying and/or by modifying the structural parameters.

A precise control of the alloying effects seems to be a good starting point for controlling the value of a_{\perp}/a_{\parallel} in these systems. The thickness and the nature of the spacer material may appear as a valuable parameter in order to control or amplify the anchoring of the magnetization of the multilayers in the different crystallographic directions. The nature of the substrate and its lattice spacing, mostly responsible for the value of the in-plane lattice parameter of the multilayers, can also be considered as a potential degree of freedom to design the a_{\perp}/a_{\parallel} ratio. However, our present analysis indicates that hybridization, structural distortion, volume expansion, and band-filling effects are all important competing effects aiming at fixing the amplitude and the sign of the MAE.

ACKNOWLEDGMENTS

The authors wish to acknowledge the support from the TMR program, and for the Swedish Natural Science Foundation (VR), as well as from the Göran Gustafsson Foundation and the Swedish Foundation for Strategic Research (SSF). We are grateful to Dr. J.M. Wills for supplying the FP-LMTO code.

APPENDIX: DEPENDENCE OF THE MAE WITH RESPECT TO THE FERMI ENERGY

The MAE calculated for a given $E_F + \delta E_F$ Fermi energy is

$$E_{a_{(E_F + \delta E_F)}} = \int_{-\infty}^{E_F + \delta E_F + \delta e} \epsilon D^{[100]}(\epsilon) d\epsilon - \int_{-\infty}^{E_F + \delta E_F} \epsilon D^{[001]}(\epsilon) d\epsilon, \quad (\text{A1})$$

where δe is the shift on the Fermi energy which gives $N_{(E_F + \delta E_F)}^{[100]} = N_{(E_F + \delta E_F)}^{[001]}$, insuring that the total charge is the same for the [100] and [001] spin directions. This shift is calculated from

$$\int_{E_F + \delta E_F}^{E_F + \delta E_F + \delta e} D^{[100]}(\epsilon) d\epsilon = -N_{(E_F + \delta E_F)}^{[100]} + N_{(E_F + \delta E_F)}^{[001]}. \quad (\text{A2})$$

Equation (A1) can be decomposed into

$$E_{a_{(E_F + \delta E_F)}} = E_{a_{(E_F)}} - \int_{E_F}^{E_F + \delta e'} \epsilon D^{[100]}(\epsilon) d\epsilon + \int_{E_F}^{E_F + \delta E_F} \epsilon \delta D(\epsilon) d\epsilon + \int_{E_F + \delta E_F}^{E_F + \delta E_F + \delta e} \epsilon D^{[100]}(\epsilon) d\epsilon, \quad (\text{A3})$$

where $\delta e'$ is the shift which gives $N_{(E_F)}^{[100]} = N_{(E_F)}^{[001]}$. δe , $\delta e'$, and δE_F being very small quantities, these integrals can be approximated by a finite summation. Equation (A3) becomes

$$E_{a_{(E_F + \delta E_F)}} = E_{a_{(E_F)}} - \delta e' E_F D_{(E_F)}^{[100]} + \delta E_F E_F \delta D_{(E_F)} + \delta e (E_F + \delta E_F) D_{(E_F + \delta E_F)}^{[100]}. \quad (\text{A4})$$

In the same manner, δe , and $\delta e'$ can be approximated by $\delta e = \delta N_{(E_F + \delta E_F)} / D_{(E_F + \delta E_F)}^{[100]}$ and $\delta e' = \delta N_{(E_F)} / D_{(E_F)}^{[100]}$, so that we have

$$E_{a_{(E_F + \delta E_F)}} = E_{a_{(E_F)}} + E_F (\delta E_F \delta D_{(E_F)} + \delta N_{(E_F)}) - (E_F + \delta E_F) \delta N_{(E_F + \delta E_F)}, \quad (\text{A5})$$

where $\delta D_{(\epsilon)}$ is defined by $D_{(\epsilon)}^{[100]} - D_{(\epsilon)}^{[001]}$, and $\delta N_{(\epsilon)} = -N_{(\epsilon)}^{[100]} + N_{(\epsilon)}^{[001]}$. At the first order in δE_F , we have $N_{(E_F + \delta E_F)} = N_{(E_F)} + \delta E_F D_{(E_F)}$, so that we obtain the following expression for $\delta N_{(E_F + \delta E_F)}$:

$$\delta N_{(E_F + \delta E_F)} = \delta N_{(E_F)} + \delta E_F \delta D_{(E_F)}. \quad (\text{A6})$$

By introducing Eq. (A6) into Eq. (A5), we finally have

$$E_{a_{(E_F + \delta E_F)}} = E_{a_{(E_F)}} - \delta E_F \delta N_{(E_F)} + O(\delta E_F^2), \quad (\text{A7})$$

which corresponds to Eq. (3.6) when presented in an integral form.

¹P. Grünberg, R. Schreiber, Y. Pang, M. B. Brodsky, and H. Sowers, Phys. Rev. Lett. **57**, 2442 (1986).

²M. N. Baibich, J. M. Broto, A. Fret, F. Nguyen Van Dau, F. Petroff, P. Etienne, G. Creuzet, A. Friederich, and J. Chazelas, Phys. Rev. Lett. **61**, 2472 (1988).

³H. Brooks, Phys. Rev. **58**, 909 (1940).

⁴G. Fletcher, Proc. R. Soc. London, Ser. A **67**, 505 (1954).

⁵H. J. F. Jansen, Phys. Rev. B **38**, 8022 (1988).

⁶G. H. O. Daalderop, P. J. Kelly, and M. F. H. Schuurmans, Phys. Rev. B **41**, 11 919 (1990).

⁷J. Trygg, B. Johansson, O. Eriksson, and J. M. Wills, Phys. Rev. Lett. **75**, 2871 (1995).

⁸G. Y. Guo, D. J. Roberts, and G. A. Gehring, Phys. Rev. B **59**, 14 466 (1999).

⁹G. Y. Guo, W. Temmerman, and H. Ebert, J. Phys.: Condens. Matter **3**, 8205 (1991).

- ¹⁰G. Y. Guo, W. Temmerman, and H. Ebert, *J. Magn. Magn. Mater.* **104-107**, 1772 (1992).
- ¹¹G. H. O. Daalderop, P. J. Kelly, and M. F. H. Schuurmans, *Phys. Rev. B* **50**, 9989 (1994).
- ¹²D. S. Wang, R. Wu, and A. J. Freeman, *Phys. Rev. Lett.* **70**, 869 (1993).
- ¹³J. Dorantes-Dávila and G. M. Pastor, *Phys. Rev. Lett.* **77**, 4450 (1996).
- ¹⁴O. Eriksson, in *Electronic Structure and Magnetism*, edited by W. Nolting (Springer-Verlag, Berlin, in press).
- ¹⁵M. Farle, A. N. Anisimov, K. Baberschke, J. Langer, and H. Malotta, *Europhys. Lett.* **49**, 658 (2000).
- ¹⁶J. M. Wills, O. Eriksson, and M. Alouani, in *Electronic Structure and Physical Properties of Solids*, edited by Hugues Dreyse (Springer-Verlag, Berlin, 2000), p. 148.
- ¹⁷L. Hedin and B. I. Lundqvist, *J. Phys. C* **4**, 2064 (1971).
- ¹⁸M. Methfessel and A. T. Paxton, *Phys. Rev. B* **40**, 3616 (1989).
- ¹⁹P. Pouloupoulos, P. Isberg, W. Platow, W. Wisny, M. Farle, B. Hjörvarsson, and K. Baberschke, *J. Magn. Magn. Mater.* **170**, 57 (1997).
- ²⁰L. C. Duda, P. Isberg, S. Mirbt, J. H. Guo, B. Hjörvarsson, J. Nordgren, and P. Granberg, *Phys. Rev. B* **54**, 10 393 (1996).
- ²¹A. N. Anisimov, W. Platow, P. Pouloupoulos, W. Wisny, M. Farle, K. Baberschke, P. Isberg, B. Hjörvarsson, and R. Wäppling, *J. Phys.: Condens. Matter* **9**, 10 581 (1997).
- ²²O. K. Andersen, H. L. Skriver, and B. Johansson, *Pure Appl. Chem.* **52**, 93 (1979); A. R. Mackintosh and O. K. Andersen, in *Electrons at the Fermi Surface*, edited by M. Springford (Cambridge University Press, Cambridge, 1980).
- ²³R. Wu, L. Chen, and A. J. Freeman, *J. Magn. Magn. Mater.* **170**, 103 (1997).
- ²⁴O. K. Andersen, *Phys. Rev. B* **12**, 3060 (1975); H. Skriver, *The LMTO Method* (Springer, Berlin, 1984).
- ²⁵A. N. Anisimov, M. Farle, P. Pouloupoulos, W. Platow, K. Baberschke, P. Isberg, R. Wäppling, A. M. N. Niklasson, and O. Eriksson, *Phys. Rev. Lett.* **82**, 2390 (1999).
- ²⁶O. Le Bacq, O. Eriksson, and A. Delin (unpublished).